Supplementary Information (SI) for Inorganic Chemistry Frontiers.
This journal is © the Partner Organisations 2024

Supporting Information for

Ultrafine cucurbit[n]uril (n = 5-8)-Ni nanocomposites as highly efficient catalysts for electrocatalytic oxygen evolution reaction

Yu-Ting Liu,†[a] Quan-Jiang Lv,†[c] Hang Cong,[a] Wen-Feng Zhao,[a] Qing-Mei Ge,[a] Nan Jiang,*[a] and Qi-Long Zhu*[b,d]

[a] *School of Chemistry and Chemical Engineering, Guizhou University, Guiyang 550025, Guizhou, China. E-mail: njiang@gzu.edu.cn.*

[b] *Fujian Science & Technology Innovation Laboratory for Optoelectronic Information of China, Fuzhou 350108, China. E-mail: qlzhu@fjirsm.ac.cn.*

[c] *School of Materials Science and Engineering, Jiangsu University, Zhenjiang 212013, Jiangsu, China.*

[d] *State Key Laboratory of Structural Chemistry, Fujian Institute of Research on the Structure of Matter, Chinese Academy of Sciences (CAS), Fuzhou 350002, Fujian, China.*

*Corresponding authors: Nan Jiang and Qi-Long Zhu

E-mail: njiang@gzu.edu.cn; qlzhu@fjirsm.ac.cn

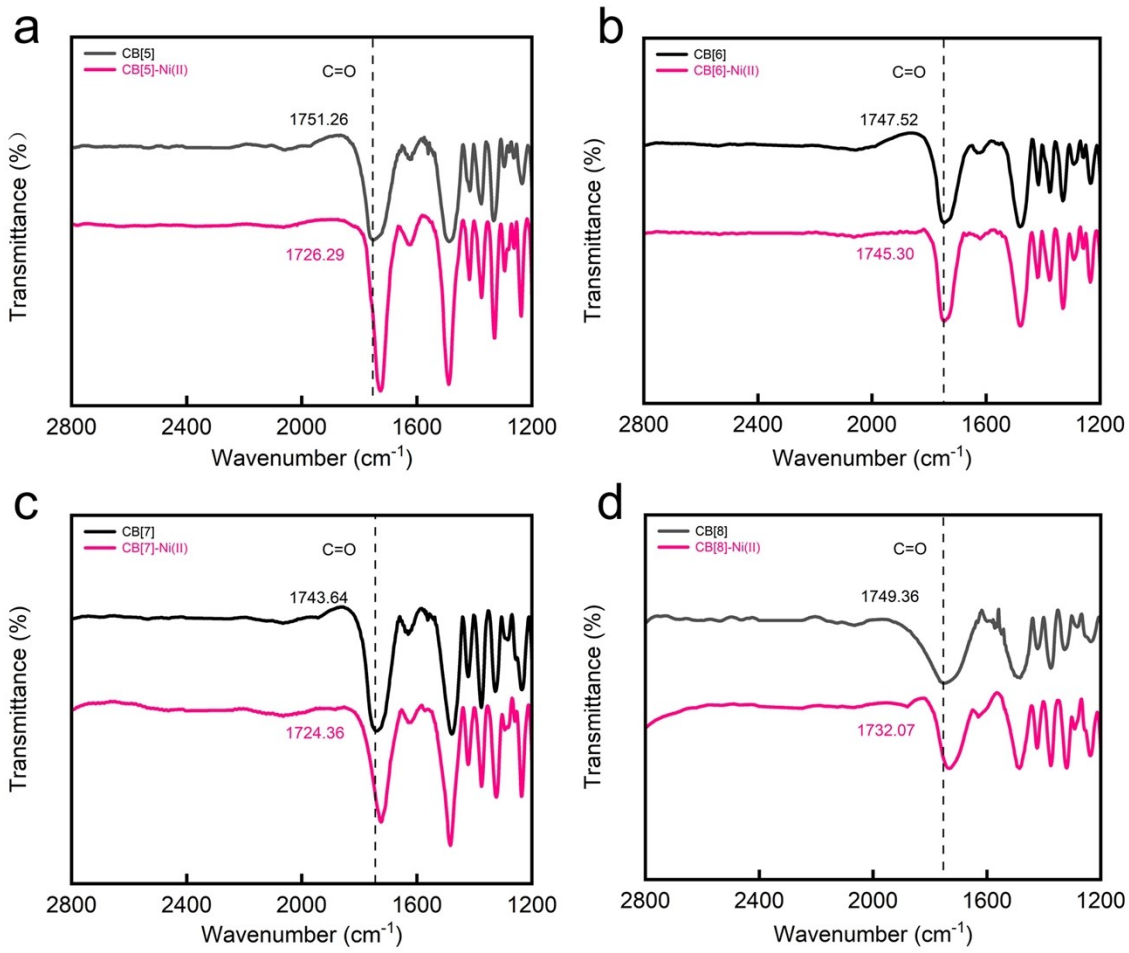

Fig. S1 FT-IR spectra of (a) CB[5] and CB[5]-Ni(II), (b) CB[6] and CB[6]-Ni(II), (c) CB[7] and CB[7]-Ni(II), (d) CB[8] and CB[8]-Ni(II).

Table. S1 The loading mass and average nanoparticle sizes of CB[n]-Ni and CB-free Ni nanocomposites.

Catalysts	CB[5]-Ni	CB[6]-Ni	CB[7]-Ni	CB[8]-Ni	CB-free Ni
Loading mass (wt%)	7.95	5.96	5.72	3.20	-
Average size (nm)	2.03	4.15	1.84	2.90	55.79

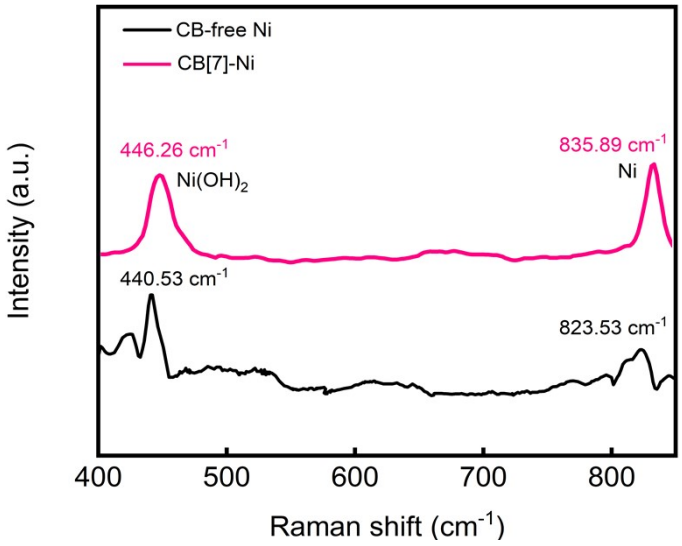

Fig. S2 Raman spectra of CB-free Ni and CB[7]-Ni.

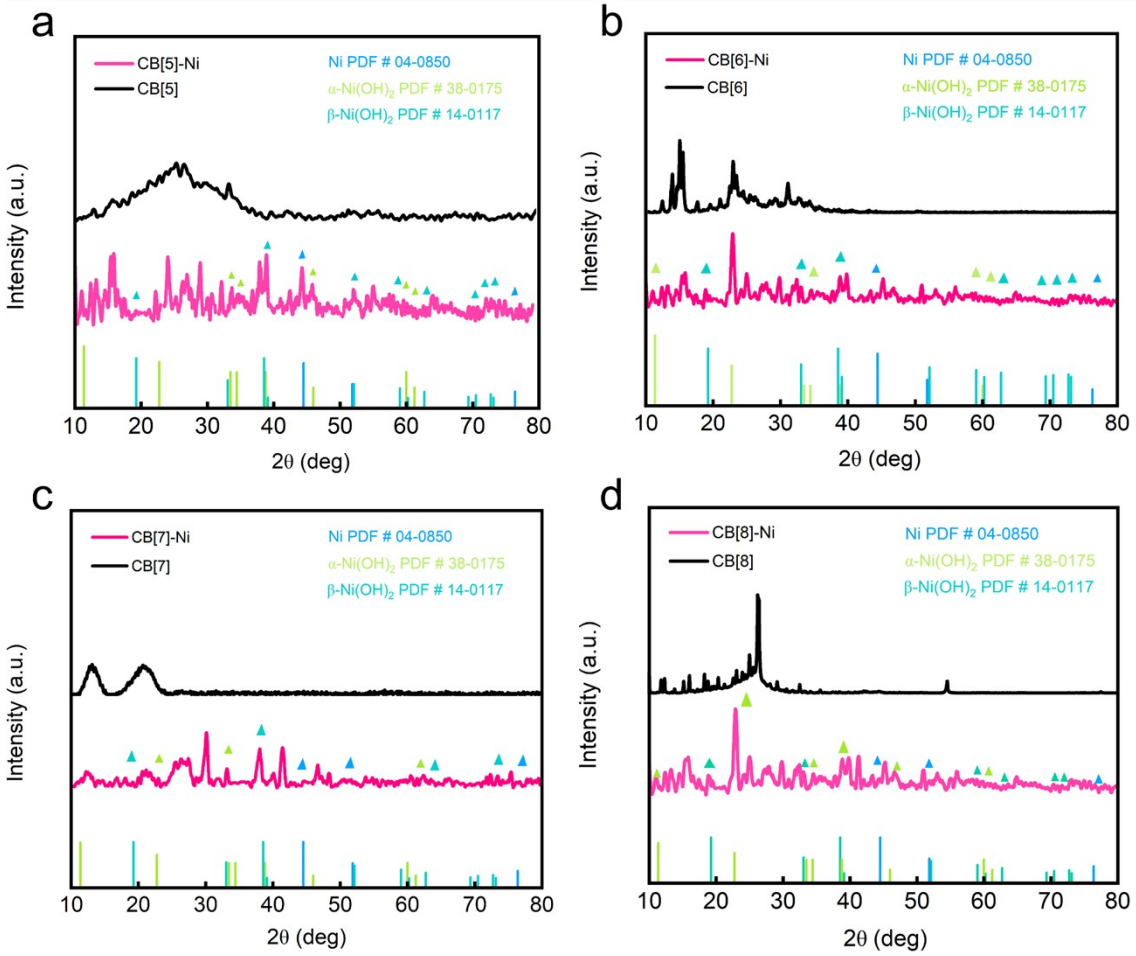

Fig. S3 XRD patterns of (a) CB[5] and CB[5]-Ni, (b) CB[6] and CB[6]-Ni, (c) CB[7] and CB[7]-Ni, (d) CB[8] and CB[8]-Ni.

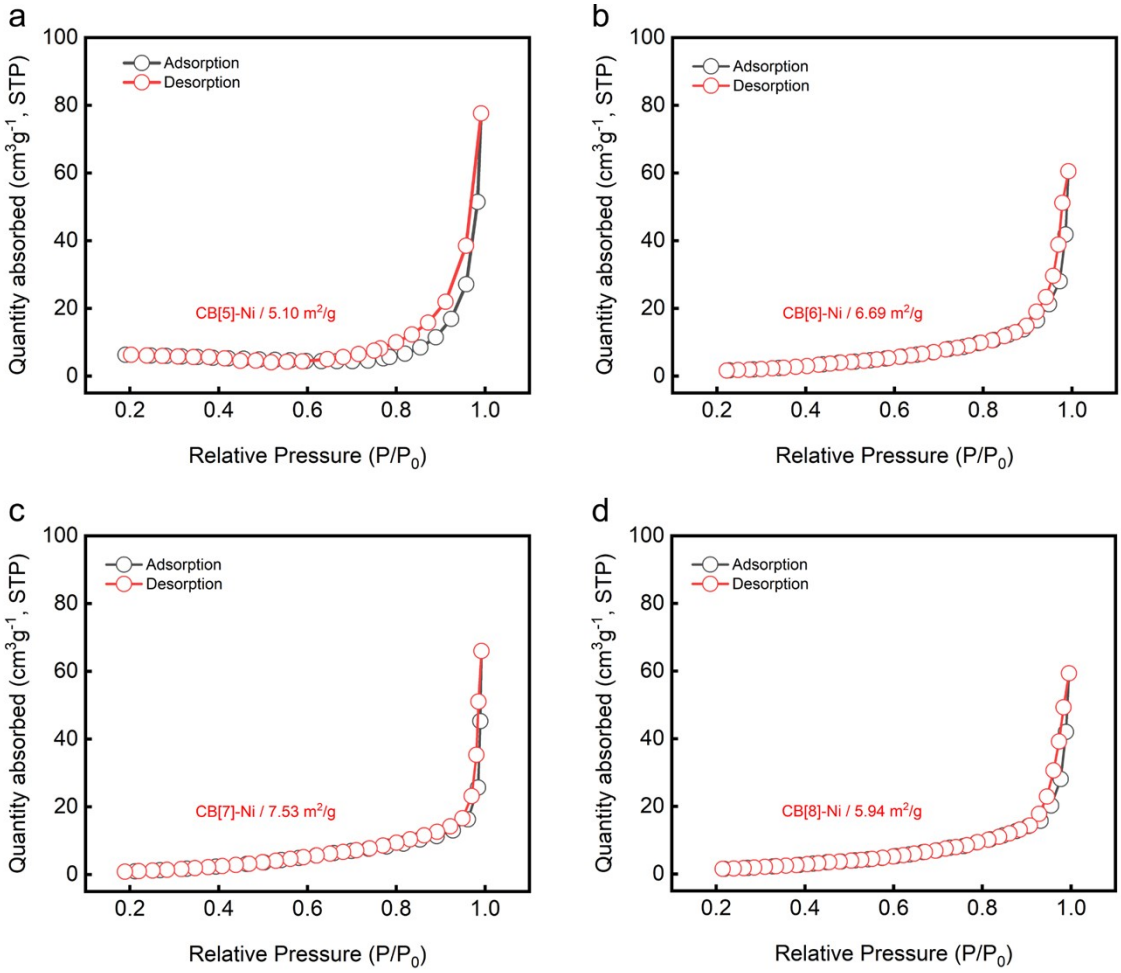

Fig. S4 N_2 sorption at 77 K of (a) CB[5]-Ni, (b) CB[6]-Ni, (c) CB[7]-Ni, and (d) CB[8]-Ni.

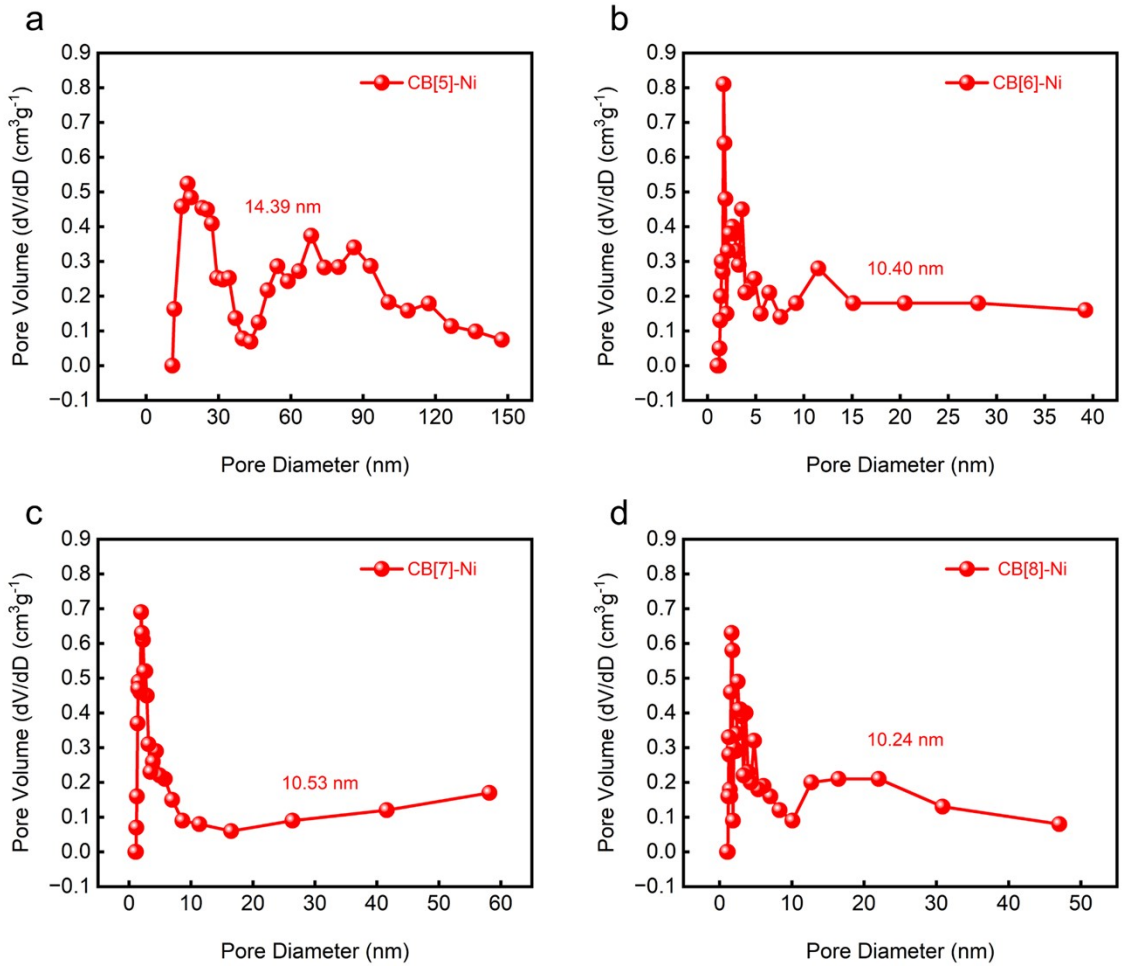

Fig. S5 Pore size distributions of (a) CB[5]-Ni, (b) CB[6]-Ni, (c) CB[7]-Ni, and (d) CB[8]-Ni.

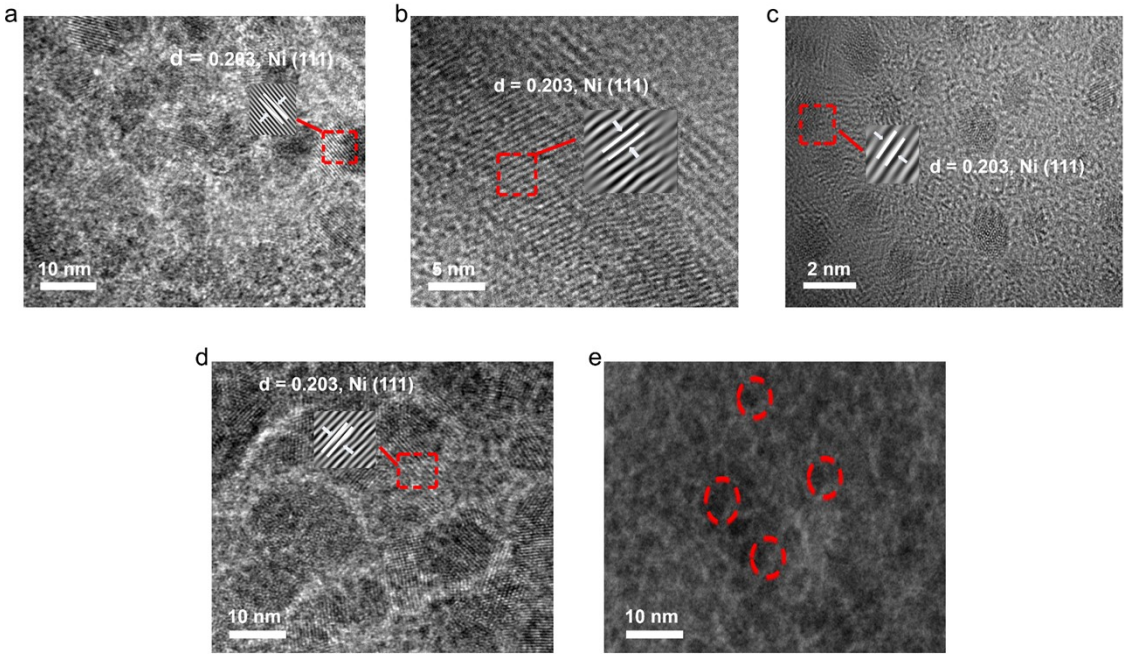

Fig. S6 HRTEM images of (a) CB[5]-Ni, (b) CB[6]-Ni, (c) CB[7]-Ni, and (d) CB[8]-Ni. (e) TEM image of CB[7]-Ni with different representative areas.

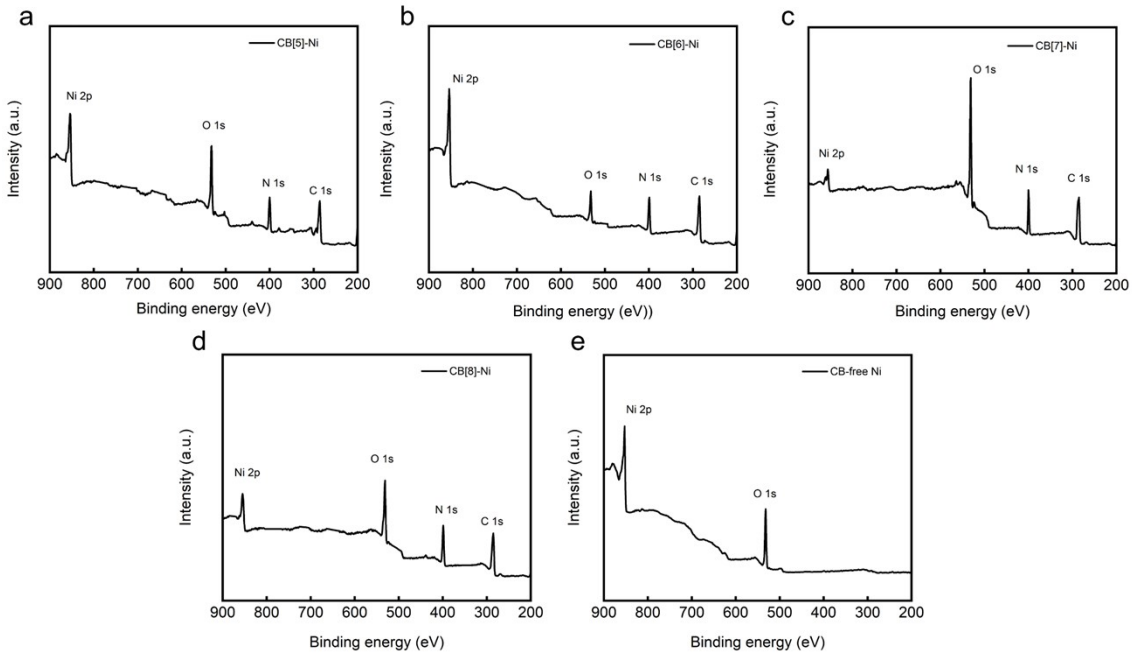

Fig. S7 XPS surveys of (a) CB[5]-Ni, (b) CB[6]-Ni, (c) CB[7]-Ni, (d) CB[8]-Ni, and (e) CB-free Ni.

Table. S2 The Ni^0/Ni^{2+} atomic ratios of CB[5]-Ni, CB[6]-Ni, CB[7]-Ni, CB[8]-Ni, and CB-free Ni nanocomposites.

Catalysts	CB[5]-Ni	CB[6]-Ni	CB[7]-Ni	CB[8]-Ni	CB-free Ni
Ni^0/Ni^{2+} atomic ratios	1.24	0.83	1.25	0.55	1.28

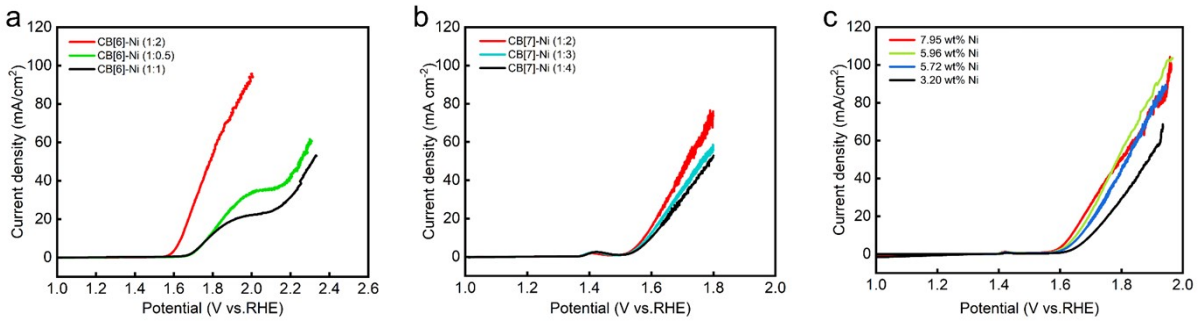

Fig. S8 (a) LSV curves of CB[6]-Ni (1:2), CB[6]-Ni (1:0.5), and CB[6]-Ni (1:1). (b) LSV curves of CB[7]-Ni (1:2), CB[7]-Ni (1:3), and CB[7]-Ni (1:4). (c) LSV curves of the catalysts with different Ni loading amounts, corresponding to CB[5]-Ni, CB[6]-Ni, CB[7]-Ni, and CB[8]-Ni.

Table. S3 Comparison of OER activities for different Ni-based electrocatalysts in 0.1 M KOH.

Catalysts	Catalyst loading (mg/cm^2)	η_{10} (mV)	Tafel slope (mV/dec)	TOF (s^{-1})	Ref
CB[7]-Ni	0.12	320	75	0.24 s^{-1} at 320 mV	This work
NiCo@N-C	0.4	530	98	--	[1]
CoNi-NCNTs	0.71	360	193	--	[2]
Ni-Co-Fe Hydroxides	0.26	250	31	0.17 s^{-1} at 300 mV	[3]
NiCo LDH@HOS	0.45	293	72	0.008 s^{-1} at 300 mV	[4]
$Co_{0.75}Ni_{0.25}Fe_2O_4$/rGO	0.23	440	85	--	[5]
NiO dots/a-carbon	0.204	296	51	--	[6]
CoNi MOF-74	0.2	300	65.6	0.0267 s^{-1} at 300 mV	[7]
N/S-RCQD@$NiCo_2S_4$	0.26	390	85.6	0.113 s^{-1} at 420 mV	[8]
CO/NCO/NF	--	320	84	0.0287 s^{-1} at 350 mV	[9]

Table. S4 Detail information of EIS fitting data at 1.66 V vs. RHE.

Equivalent circuit	Sample	R_s (Ω)	CPE (F/cm^2)	R_{ct} (Ω)
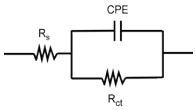	CB[5]-Ni	22.23	0.00367	13.79
	CB[6]-Ni	21.15	0.005046	8.86
	CB[7]-Ni	19.17	0.005655	6.89
	CB[8]-Ni	26.22	0.0002893	14.52
	CB-free Ni	34.15	0.0001779	22.74

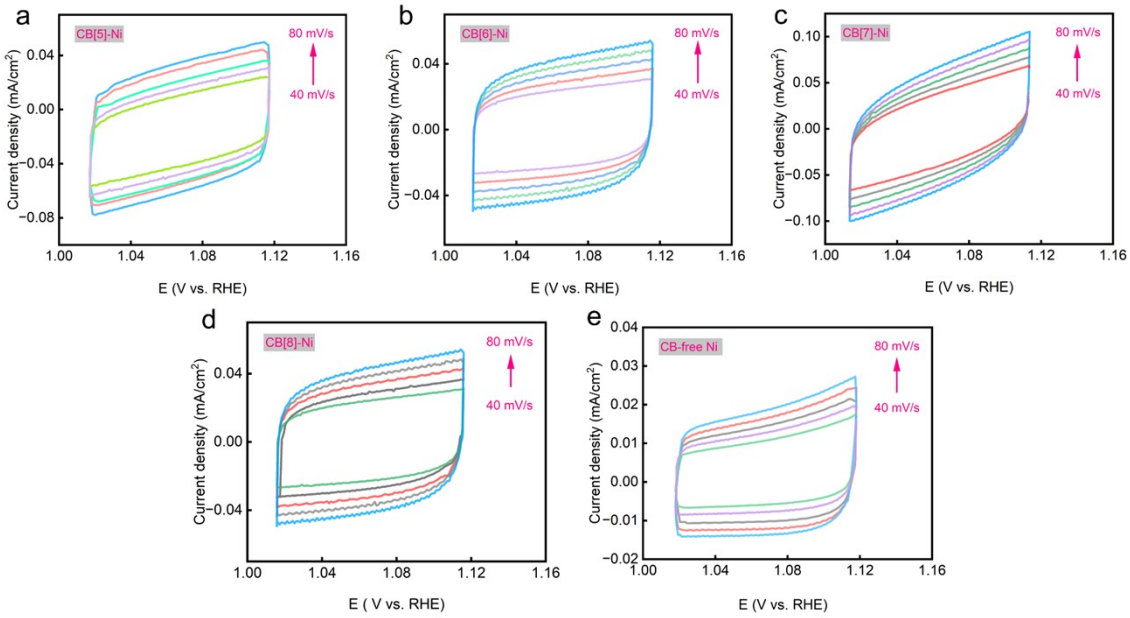

Fig. S9 CV plots at different scan rates of (a) CB[5]-Ni, (b) CB[6]-Ni, (c) CB[7]-Ni, (d) CB[8]-Ni, and (e) CB-free Ni nanocomposites.

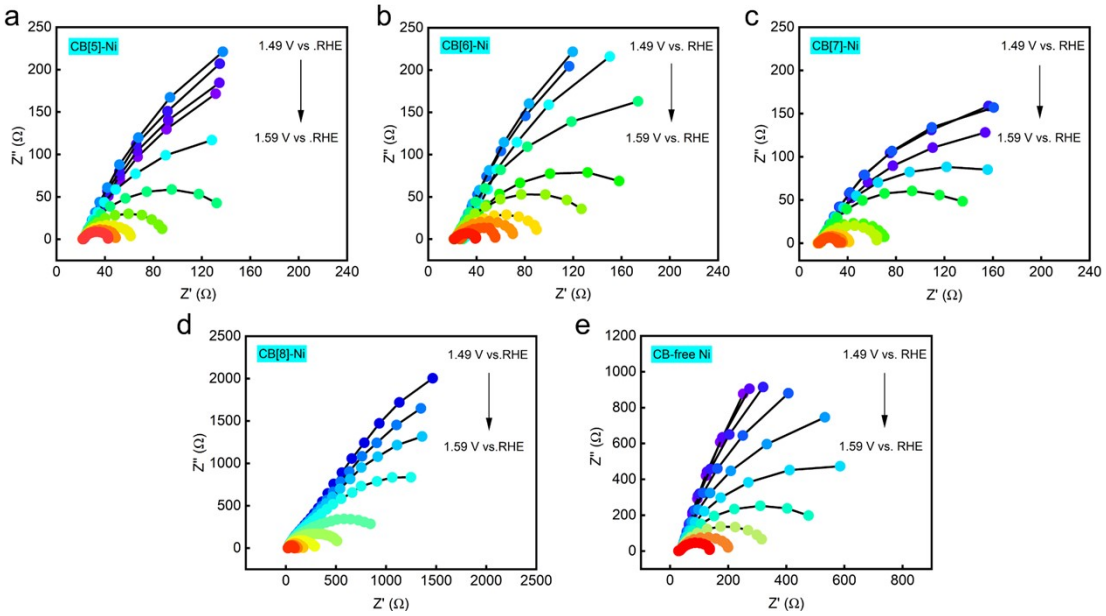

Fig. S10 Nyquist plots of (a) CB[5]-Ni, (b) CB[6]-Ni, (c) CB[7]-Ni, (d) CB[8]-Ni, and (e) CB-free Ni nanocomposites at different applied potentials.

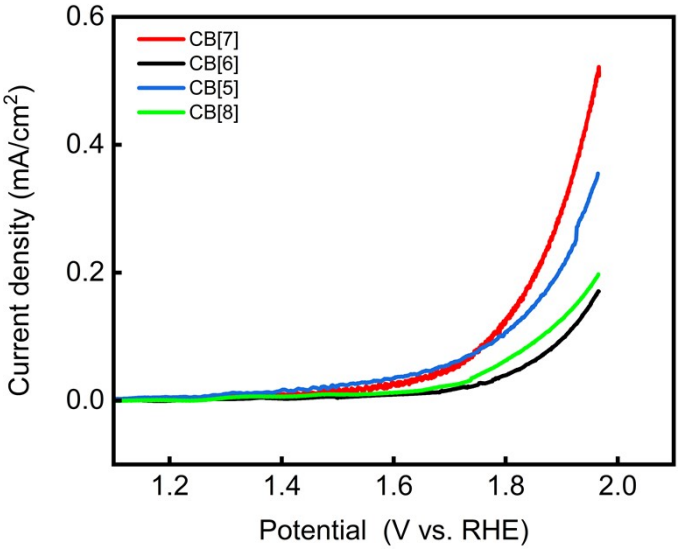

Fig. S11 LSV curves of the pure CB[n] in 0.1 M KOH.

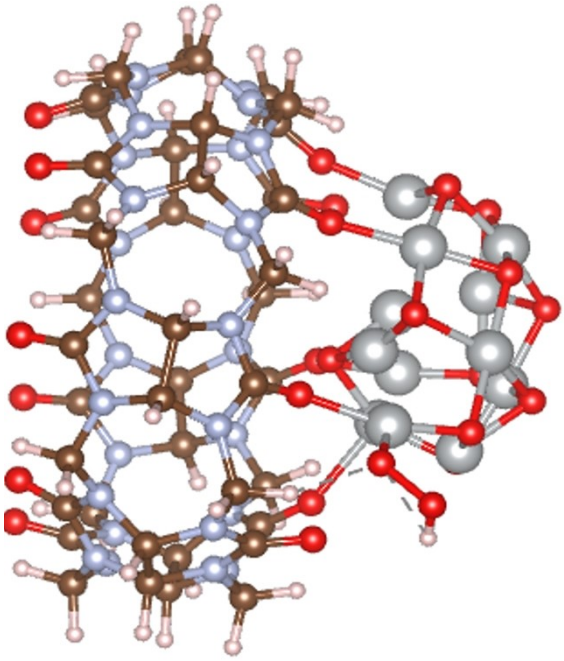

Fig. S12 Stable state of the adsorption of CB[7] on $Ni_{12}O_{10}H_5$.

Table. S5 The calculated C=O bond length data from DFT.

Samples	C=O bond length (Å)	Adsorption energy (kcal/mol)
CB[5]	1.219	-
CB[5]-Ni	1.227	9.38
CB[6]	1.220	-
CB[6]-Ni	1.233	8.50
CB[7]	1.220	-
CB[7]-Ni	1.234	12.81
CB[8]	1.221	-
CB[8]-Ni	1.231	12.06

Table. S6 Adsorption energies of *OOH intermediates on CB[n]-Ni and CB-free Ni.

Catalyst	CB[5]-Ni	CB[6]-Ni	CB[7]-Ni	CB[8]-Ni	CB-free Ni
Adsorption energy (kcal/mol)	6.99	6.11	5.18	7.64	8.37

Reference:

1. Y. Fu, H.-Y. Yu, C. Jiang, T.-H. Zhang, R. Zhan, X. Li, J.-F. Li, J.-H. Tian and R. Yang, NiCo alloy nanoparticles decorated on N-doped carbon nanofibers as highly active and durable oxygen electrocatalyst, *Adv. Funct. Mater.*, 2018, **28**, 1705094.

2. Y. Hou, S. Cui, Z. Wen, X. Guo, X. Feng and J. Chen, Strongly coupled 3D hybrids of N-doped porous carbon nanosheet/CoNi alloy-encapsulated carbon nanotubes for enhanced electrocatalysis, *Small*, 2015, **11**, 5940-5948.

3. W.-J. Liu, X. Hu, H.-C. Li and H.-Q. Yu, Pseudocapacitive Ni-Co-Fe hydroxides/N-doped carbon nanoplates-based electrocatalyst for efficient oxygen evolution, *Small*, 2018, **14**, 1801878.

4. K. Xiang, J. Guo, J. Xu, T. Qu, Y. Zhang, S. Chen, P. Hao, M. Li, M. Xie, X. Guo and W. Ding, Surface sulfurization of NiCo-layered double hydroxide nanosheets enable superior and durable oxygen evolution electrocatalysis, *ACS. Appl. Ener. Mater.*, 2018, **1**, 4040-4049.

5. I. Madakannu, I. Patil, B. A. Kakade and K. R. D. Kasibhatta, Boosting oxygen evolution reaction performance by nickel substituted cobalt-iron oxide nanoparticles embedded over reduced graphene oxide, *Mater. Chem. Phys.*, 2020, **252**, 123238.

6. B. Jin, Q. Wang, J. Sainio, V. A. Saveleva, H. Jiang, J. Shi, B. Ali, A.-J. Kallio, S. Huotari, D. Sundholm, N. Han and T. Kallio, Amorphous carbon modulated-quantum dots NiO for efficient oxygen evolution in anion exchange membrane water electrolyzer, *Appl. Cata. B.*, 2024, **358**, 124437.

7. F. Sun, H. Xu, W. Zhu, C. Lu, L. Ren, L. Chong and J. Zou, Bimetal metal-organic framework hollow nanoprisms for enhanced electrochemical oxygen evolution, *Int. J. Hydrogen Energy*, 2023, **48**, 3942-3951.

8. M. S. Amjadi, H. Ashassi-Sorkhabi, M. G. Hosseini, B. G. Pollet and E. Asghari, N/S-RCQD@$NiCo_2S_4$ nanocomposite with wrinkled nanosheet-like edges as an anode for water splitting, *J. Energy Storage*, 2023, **72**, 108364.

9. M. Yang, W. Lu, R. Jin, X.-C. Liu, S. Song and Y. Xing, Superior oxygen evolution reaction performance of Co_3O_4/$NiCo_2O_4$/Ni foam composite with hierarchical structure, *ACS. Sustain. Chem. Eng.*, 2019, **7**, 12214-12221.